Design of Patchy Particles Using Quaternary Self-Assembled Monolayers

Ines C. Pons-Siepermann[†] and Sharon C. Glotzer[†,‡,*]

[†]Department of Chemical Engineering and [‡]Department of Materials Science & Engineering, University of Michigan, 2300 Hayward Street, 3406 G.G. Brown Building, Ann Arbor, Michigan 48109, United States

ABSTRACT

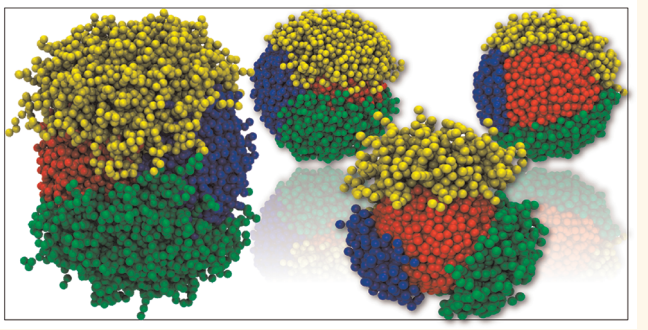

Binary and ternary self-assembled monolayers (SAMs) adsorbed on gold nanoparticles (NPs) have been previously studied for their propensity to form novel and unexpected patterns. The patterns found were shown to arise from a competition between immiscibilty of unlike surfactants and entropic gains due to length or other architectural differences between them. We investigate patterns self-assembled from quaternary monolayers on spherical nanoparticles. We perform simulations to study the effect of NP radius, degree of immiscibility between surfactants, length differences, and stoichiometry of the SAM on the formation of patterns. We report patterns analogous to binary and ternary cases, as well as some novel patterns specific to quaternary SAMs.

KEYWORDS: patchy particles · self-assembly · quaternary · phase separation · dissipative particle dynamics

Previous experimental[1−7] and computational[8−13] studies investigated the formation of patterns on monolayer-protected metal nanoparticles (MPMNPs) consisting of a gold nanoparticle covered by a self-assembled monolayer (SAM) formed by a binary mixture of immiscible (different end groups) thiol surfactants. They found that when the length difference between the immiscible surfactants is sufficient, the SAMs form a striped pattern on the surface of the NP; otherwise the surfactants phase separate on the surface, producing a Janus particle.[8] These patterns were predicted on both spherical[9] and rod-shaped[13] NPs. In all cases, pattern formation was shown to be dictated by a competition between energy minimization, which tends to minimize contact between immiscible surfactants, and maximization of conformational entropy gained by forming interfaces between surfactants of different length or bulkiness.

In a recent computational study we extended those investigations to patterns formed on ternary MPMNPs.[14] We found that by adding a third surfactant to the mixture we could increase the number and diversity of possible patterns and select for these patterns based on easy-to-control parameters such as NP radius and surfactant length, as well as less-easy-to-control parameters such as degree of immiscibility among surfactants and stoichiometry of the SAM. Here we present the results of adding a fourth surfactant to the monolayer, forming a quaternary mixture of different surfactants. We consider the effect of tuning the parameters mentioned above, while always considering four immiscible ligands, and show that although some patterns are natural analogues of binary and ternary patterns, new and unexpected patterns due solely to the addition of a fourth ligand are possible. Although finding suitable ligands may prove challenging experimentally, we note that mixtures of up to five ligands have been reported.[15]

RESULTS AND DISCUSSION

We find different patterns for the quaternary SAMs depending on combination of parameters. Figure 1 shows the generalized types of patterns found. We describe each of these patterns below. As we will show, many of these patterns can be further decorated by modifying additional parameters.

Tetrahedral Particles. Figure 1a shows a patchy particle with tetrahedral symmetry in the SAM pattern. We refer to this particle as a tetrahedral particle. This pattern minimizes the interface between all surfactant pairs. Moreover, the three longest surfactants (shown in blue, green, and yellow) all have an interface with the shortest surfactant (shown in red in the leftmost image in

* Address correspondence to sglotzer@umich.edu.

Received for review January 5, 2012 and accepted April 26, 2012.

Published online 10.1021/nn300059x

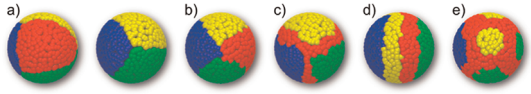

Figure 1. Generalized patterns predicted for quaternary MPMNPs: (a) tetrahedral, (b) Brahma, (c) decorated Cerberus, (d) decorated stripes, and (e) spots. Tails are not shown. Red: short, blue: medium, green: long, and yellow: longest surfactant. All particles shown look identical when viewed from the opposite side of that shown, with the exception of the tetrahedral particle in (a), where the second view is shown.

Figure 1a). When viewed from the top, this particle looks exactly like a Cerberus particle found in the ternary systems[14] shown in the rightmost image in Figure 1a. The tetrahedral particle forms in cases when the surfactants are very long compared to the NP radius (*i.e.*, all surfactants are at least 10 beads long, for a NP radius of 4), but the length difference between the four surfactants is relatively small (no more than six beads difference between the shortest and longest surfactants).

Brahma Particles. Figure 1b shows a patchy particle with the SAM separated into equal quadrants; we refer to this particle as the Brahma particle, in reference to the Hindu god of creation, who is traditionally depicted with four heads. Here the surfactants again separate without forming stripes, but now each surfactant forms an interface with only two of the others. The two longest surfactants (shown in yellow and green) do not share an interface, and both form an interface with the two shortest surfactants (shown in red and green). This pattern forms when the SAM comprises two short and two long surfactants (*i.e.*, the surfactants are 5, 6, 13, and 14 beads long, respectively, for a NP of radius 4).

Decorated Cerberus Particles. We observe several types of patterns where three of the surfactants segregate into dominant features. Figure 1c shows an example of one such "Cerberus" particle. Additional details of additional Cerberus patterns predicted by our simulations are shown in Figure 2. Figure 2a shows a Cerberus NP decorated with a stripe of the shortest surfactant (shown in red) separating the three longest ones. We observe this particular pattern when the system has one short surfactant and three long ones (*i.e.*, 3, 7, 8, and 9 beads) and the repulsion between unlike surfactants is low (a_{ij} = 30). In this case, all three long surfactants compete to form an interface with the short one to maximize the free volume available for their tails to explore.

Figure 2b shows a similar case, with the difference that the longest surfactant (shown in yellow) is separated from all others by the short one (shown in red), while the two medium length surfactants (shown in blue and green) share an interface. This pattern also forms when there is one short surfactant in the system and three long ones (*i.e.*, 3, 7, 8, and 9 beads) but when the interbead repulsion between unlike surfactants is

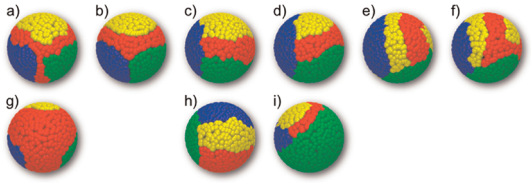

Figure 2. Decorated Cerberus patterns. Tails are not shown. Red: short, blue: medium, green: long, and yellow: longest surfactant. (a) through (f) show different patterns. (a) and (g) and also (d) and (i) show the same type of pattern but obtained with different stoichiometric compositions. (c) and (h) also show the same pattern, but with different chemical ordering due to different combinations of surfactant lengths.

high (a_{ij} = 65). In this case the system's free energy is minimized by minimizing the number of interactions between the longest (yellow) and the two medium surfactants (blue and green).

Figure 2c is again similar to Figure 2b, with the difference that the short surfactant (red) separates only the two longest ones (green and yellow). Both of these long surfactants have an interface with the medium one (blue). This pattern forms when the surfactants have an equal length difference (*i.e.*, 3, 5, 7, and 9 beads) and the interbead repulsion between unlike surfactants is high (a_{ij} = 65). Since the medium surfactant (blue) is relatively short compared to the two longest ones (green and yellow), both of them gain conformational entropy by forming an interface with it.

An analogous pattern to Figure 2c is shown in Figure 2h. However, the arrangement of the surfactants is not the same between these two patterns. Figure 2h occurs when there are three short and one long surfactant in the system (*i.e.*, 3, 4, 5, and 11 beads) and the interbead repulsion between unlike beads is high (a_{ij} = 65). In this case, the longest surfactant (yellow) maximizes its interface with the two shortest (red and blue) and also has a smaller interface with the second longest (green).

Figure 2d is similar to Figure 2c, with the difference that the stripe formed by the short surfactant (red) curves toward the longest (yellow) surfactant to increase the length of the interface between the two longest surfactants (in green and yellow) and the shortest one (in red). This pattern is obtained for SAMs formed by surfactants of symmetric lengths (*i.e.*, 3, 5, 7, and 9 beads) and low interbead repulsion between unlike surfactants (a_{ij} = 30). Therefore, this pattern occurs under conditions similar to Figure 2c, with the only difference that the interbead repulsion between unlike surfactants is smaller for Figure 2d, which is why the surfactants prefer to form a longer interface.

In Figure 2e the short surfactant (shown in red) forms a single stripe inside the domain of the longest surfactant (shown in yellow). The stripe also has interfaces with the second longest surfactant (shown in green), but none with the medium surfactants

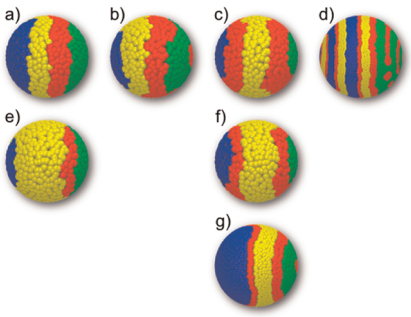

Figure 3. Decorated striped patterns. Tails are not shown. Red: short, blue: medium, green: long, and yellow: longest surfactant. (a) through (d) show different patterns. (a) and (e) and also (c) and (f) show the same pattern but obtained with different stoichiometric compositions. (c) and (g) also show the same patterns, but (g) has an additional patch of the short surfactant (in red) inside the domain of the second longest surfactant (in green).

(shown in blue). This pattern occurs for three short surfactants (*i.e.*, 4, 5, 6, and 11 beads) when the interbead repulsion between unlike surfactants is low (a_{ij} = 30). It is similar to Figure 2h (also three short surfactants, but higher interbead repulsion) with the difference that in the case of lower interbead repulsion the long and short surfactants form additional interfaces between them.

Figure 2f is a subcase of Figure 2e, in which the stripe of the short surfactant (red) becomes a fully closed circle, creating a larger interface with the second longest surfactant (green). This case also occurs for three short surfactants and low interbead repulsion between unlike beads, but only for very short surfactants with respect to the NP radius (3, 4, and 5 beads long for the shortest surfactants, up to 9 beads long for the longest).

Some of the Cerberus patterns shown in Figure 2 can be further modified by introducing variations in the stoichiometric composition of the SAM, as shown in Figure 2g and i. The patterns shown in Figure 2a and d result from a 1:1:1:1 stoichiometry. These patterns are also shown in Figure 2g and i, but for different stoichiometric compositions. Figure 2g shows the case for a stoichiometric composition of 7:1:1:1, where the short surfactant (shown in red) is in excess over the other three. Figure 2i shows a stoichiometric composition of 1:1:6:2.

Decorated Striped Particles. Several variations can be found also for the striped patterns (Figure 1d), as shown in Figure 3. Figure 3a shows the simplest case, in which the four surfactants form one single stripe around the NP. The longest surfactant (in yellow) has an interface with the two shortest ones (in red and blue). Also, the two longest surfactants (yellow and green) both have an interface with the shortest (red). This pattern is found for a system with two short surfactants (*i.e.*, 3, 4, 7, and 8 beads) and low interbead repulsion between unlike beads (a_{ij} = 30) when the overall length of the surfactants is relatively short compared to the NP size (*i.e.*, all surfactants are less than 10 beads long). This pattern is also prevalent when the two shortest surfactants are in very low concentrations (≤20% of each), an example of which is shown in Figure 3e.

Figure 3b shows a modified version of Figure 3a, where there is one additional patch of the short surfactant (in red) inside the domain formed by the second longest surfactant (green). This case occurs under a very narrow range of conditions, for a system with two short surfactants (*i.e.*, 3, 4, 8, and 9 beads) with low interbead repulsion between unlike surfactants (a_{ij} = 30) when the overall length of the surfactants is longer than the case for Figure 3a.

Figure 3c shows a striped pattern where the short surfactant (in red) forms two stripes around the NP, instead of just one. These two stripes separate the longest surfactant (in yellow) from the two medium length surfactants (in blue and green). This pattern is found for large NP radius (NP radius > 4) and high interbead repulsion between unlike beads ($65 < a_{ij} \leq 350$). In systems with large NP radius, the surfactants have less available space to explore with their tails,[17] and therefore the longest surfactant (yellow) prefers to increase its interface with the short one (red). This pattern can also be found in systems were the medium surfactant (blue) is in the lowest concentration (≤10%), so there is not enough of it available to create sufficient interfaces with the longest one (yellow).

Figure 3g is a simlar case to Figure 3c, with the only difference being that there is an additional patch of the small surfactant (in red) inside the domain formed by the second longest (in green). This pattern is found also for large NP radius, but for smaller repulsion between unlike beads (a_{ij} = 65).

Figure 3d shows a Janus NP decorated with stripes on both sides. The two shortest surfactants (in red and blue) form an alternating stripe pattern[9] with the longest surfactant (yellow) on one side of the Janus particle, while the second longest surfactant (green) forms a striped pattern with the shortest one (red) on the other side of the NP. This pattern is found for large NP radius (>4) and low interbead repulsion between unlike beads (a_{ij} = 30) and is analogous to the pattern observed under similar conditions for ternary systems.[9]

Finally, similar to the case for Cerberus patterns, we also observed variations of the striped patterns with stoichiometric changes in the SAM. Figure 3e and f are two examples of these modifications for stoichiometries 1:1:2:6 and 3:1:1:5, respectively.

Spotted Particles. Figure 1e shows a spotted patchy particle, which is found in the case where the short surfactant (in red) is in excess (>50%) of the other ones. The three longest surfactants form circular 2D micelles (spots) that are dispersed in a continuous matrix of the short one. Analogous results have been observed in the binary[16] and ternary[14] cases.

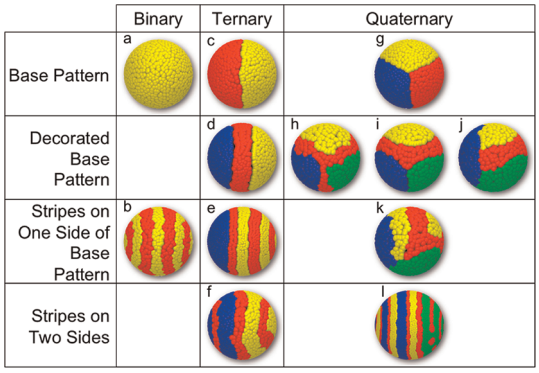

Figure 4. Comparison of binary, ternary, and quaternary patterns found on MPMNPs. Tails are not shown. Red: short, blue: medium, green: long, and yellow: longest surfactant. Binary results are recreated following refs 8, 9, and 16. Ternary results are from ref 14.

Comparison with Binary and Ternary MPMNPs. Some of the results found for quaternary MPMNPs have relatively low symmetry. To understand this unexpected behavior, we compared these patterns with those found for binary and ternary NPs in Figure 4. We discussed previously how the Cerberus and Brahma particles are the ternary and quaternary equivalents, respectively, to the Janus particle found for binary MPMNPs. In Figure 4 we also show how the Janus pattern is the base for most of the patterns found on ternary SAMs, and the Cerberus pattern is the base for most of the patterns found on quaternary SAMs. Of course, there are exceptions to this behavior, such as the alternating stripe pattern on ternary[14] SAMs and the tetrahedral, Brahma, and decorated stripe patterns on quaternary SAMs.

As shown in Figure 4, for binary MPMNPs the base pattern is a NP coated by a single surfactant (Figure 4a), and this can only be decorated with stripes on one side of the pattern (Figure 4b). However, when we move to ternary MPMNPs, we increase the number of possible options. In this case, the base pattern is a Janus particle (Figure 4c), which can be decorated with a single stripe separating the two sides of the Janus particle to form a Neapolitan particle (Figure 4d), or stripes in either one (Figure 4e) or two (Figure 4f) sides of the NP. In doing this, certain symmetries in the patterns are broken. For example, the Neapolitan pattern (Figure 4d) and the Janus pattern with stripes on both sides (Figure 4f) have higher symmetry when the difference in tail lengths is disregarded. The least symmetric pattern for ternary MPMNPs is the striped Janus NP (Figure 4e), where there are stripes on only one side of the NP.

In the case of quaternary MPMNPs, the introduction of the fourth surfactant further increases the number of possible patterns that can be constructed. The base pattern now is a Cerberus particle (Figure 4g), which is further decorated by the addition of the fourth surfactant. Analogous to the formation of Neapolitan particles (Figure 4d) for the ternary case, a stripe may separate all sides of the Cerberus particle (Figure 4h), or only two sides of the Cerberus particle (Figure 4i), or even just one side (Figure 4j). With each of these patterns, the symmetry successively decreases. Similarly, we found a quaternary pattern in which there are stripes only on one side of the NP (Figure 4k), and thus two sides without stripes.

However, instead of a Cerberus particle with stripes on two sides, which would be the quaternary equivalent of Figure 4f, we find a Janus particle with stripes on both sides (Figure 4l). In this case it is symmetry that drives the system to form this Janus particle with stripes on both sides, instead of forming a Cerberus pattern with stripes on two sides and one stripeless side. In the previous cases (Figure 4h–k) there was no option that offered more symmetry to the system, so the asymmetric patterns formed instead.

With this, it becomes clear that introducing additional surfactants in the monolayer is a way of

TABLE 1. Summary of Design Rules and Patterns for MPMNPs[a]

	Binary	Ternary	Quaternary
Small NP radius			
Base Case		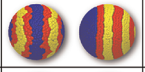	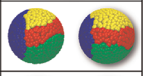
Large NP radius			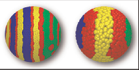
1 short surfactant			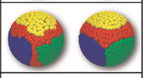
2 short surfactants			
3 short surfactants			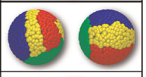
Excess of short surfactant			

[a] Tails are not shown. Red: short, blue: medium, green: long, and yellow: longest surfactant. Particles are not drawn to scale. The base case has a 1:1:1:1 stoichiometry, with symmetric length diference between surfactants (3, 6, and 9 beads for ternary; 3, 6, 9, and 12 beads for quaternary) on a NP of radius 4. In the cases when there are two images per case (*e.g.*, ternary base case) the leftmost image corresponds to weak immiscibility between unlike surfactants (a_{ij} = 30) and the rightmost corresponds to strong immiscibility between unlike surfactants (a_{ij} = 65). Shadowed in gray are cases that do not apply, based on the number of surfactants available. Additional details may be found in the Supporting Information. Binary results are recreated following refs 8, 9, and 16. Ternary results are from ref 14.

introducing additional anisotropy to the resulting MPMNPs. Since higher anisotropy of the patterns can guide increasingly more complicated assemblies of NPs, this approach to produce anisotropic building blocks could provide a novel route to obtain higher order structures not possible with high-symmetry NPs.

CONCLUSIONS

Similar to patterns found on binary and ternary MPMNPs, the patterns presented here for quaternary SAMs are all motivated by a competition between the immiscibility of the unlike surfactants driving phase separation and their length difference driving the creation of interfaces so that the longest surfactants have additional free volume available to explore. We reported motifs that are reminiscent of binary and ternary SAMs, including Cerberus, striped Janus, and spotted. Some of the other patterns found are natural extensions of patterns obtained from binary and ternary SAM MPMNPs. For example, the Brahma particle is analogous to the Janus particle for binary SAMs[8,10] and to Cerberus particles for ternary SAMS.[14] Similarly, the striped pattern for quaternary SAMs (Figure 1d) is the four-surfactant equivalent to the Neapolitan pattern found in ternary SAM MPMNPs.[14] However, some of the patterns reported here are unique to quaternary systems, such as the tetrahedral particle (Figure 1a and f) and some of the more complicatedly decorated Ceberus patterns (Figure 2e and f).

We can summarize our findings as general design rules for patchy particles made from quaternary (four-component) SAM MPMNPs:

(1) Patchy particles with tetrahedral symmetry (Figure 1a) can be obtained by using the smallest NP radius possible or by increasing the overall size of the four surfactants with respect to the NP radius, so as to optimize for "bulk" phase separation in lieu of microphase separation.

(2) Brahma NPs (Figure 1b) can be produced by using two long and two short surfactants so that there is no interface between the two longest surfactants and the two short ones assembled between them.

(3) The decorated Cerberus patterns can be obtained by various combinations of surfactant length and immiscibility between unlike surfactants, playing off phase separation and microphase separation unequally between different surfactant pairs:
- Cerberus particles analogous to those predicted for ternary MPMNPs[14] but with simple decorations between the three main domains of the NP can be obtained when there is one short surfactant and three longer ones (Figure 2a and b).
- Modified Cerberus particles in which three surfactants form three parallel stripes and the fourth forms one perpendicular stripe on a pole of the NP (Figure 2c, d, and h) can be obtained for symmetric length differences between surfactants when the overall length of the four surfactants is long with respect to the NP radius, or for three short surfactants when the unlike surfactants are strongly immiscible.
- A Cerberus particle in which there are stripes in one of the three domains (Figure 2e and f) can be made using three short and one long surfactant, with weak immiscibility between unlike surfactants.

(4) Striped particles can be achieved for weak immiscbility between unlike surfactants and can be further complicated by increasing the NP radius, going from a simple system of four stripes (Figure 3a) all the way to a decorated Janus NP with stripes on both sides of the NP (Figure 3d).

(5) Modifying the stoichiometric composition of the SAM allows one to tune the coverage of each surfactant on the surface of the NP for some of the previous patterns, except for the cases when the small surfactant is in excess of 50%, which produces a spotted pattern of 2D micelles (Figure 1e).

These design rules are summarized in Table 1 together with analogous design rules for binary and ternary SAM MPMNPs.

METHODS

We use dissipative particle dynamics (DPD),[17] a coarse-grained simulation model and method in which the surfactants are treated as chains of beads with a soft repulsion between them. This molecular-dynamics method has been used before to successfully model binary[8,11,13] and ternary[14] MPMNPs. The simulations were run using HOOMD-blue,[18–20] a highly optimized, open source GPU-based code for molecular simulations. To verify that the patterns presented in this paper correspond to the equilibrated pattern (and are not dependent on the initial configuration of the system), for each choice of parameter combinations studied we ran independent simulations from five different initial configurations (random, Brahma, and stripes of different order) for at least 30 million DPD steps. The length scale of the system was defined by the bead's diameter, which was set to 1. The radius of the NP is expressed as a function of this bead diameter, and the length of the surfactants is expressed in number of beads. The base case was considered to be a NP of radius 4 covered by a 1:1:1:1 mixture of surfactants of 3, 6, 9, and 12 beads respectively. The interbead repulsion for beads of the same surfactant (DPD parameter a_{ii}) was 15. Two base case repulsions were considered for beads of different surfactants (a_{ij}), 30 and 65. The radius of the NP was varied from 1 to 8 for interbead repulsions a_{ij} ranging from 30 to 350. All possible quaternary stoichiometries were considered for the base case. The length of the surfactants was varied from the

shortest surfactant, being 3 to 10 beads long, to the longest, being 6 to 34 beads long. Four cases were considered when varying the length of the surfactants: one short and three long surfactants (*i.e.*, 3, 8, 9, and 10 beads), two short and two long surfactants (*i.e.*, 3, 4, 9, and 10 beads), three short and one long surfactants (*i.e.*, 3, 4, 5, and 10 beads), and symmetric (*i.e.*, equivalent) length differences between all surfactants in the system (3, 5, 7, and 9 beads). To explore the effect of all the aforementioned parameters, we performed a total of 3280 production runs averaging 10 GPU-hours per run.

Conflict of Interest: The authors declare no competing financial interest.

Acknowledgment. This material is based upon work supported by the Defense Threat Reduction Agency under Grant No. HDTRA1-09-1-0012. S.C.G. is also supported by a National Security Science and Engineering Faculty Fellowship from the DOD/ASD(R&E) under Grant No. N00244-09-1-0062. Any opinions, findings, and conclusions or recommendations expressed in this material are those of the author(s) and do not necessarily reflect the views of the Defense Threat Reduction Agency or those of the DOD/ASD(R&E). I.C.P.S. and S.C.G. also acknowledge support from the James S. McDonnell Foundation 21st Century Science Research Award/Studying Complex Systems, Grant No. 220020139.

Supporting Information Available: Phase diagrams are presented for all the systems studied, to illustrate the transitions between patterns presented in the main text. Figure S1 shows the effect of NP radius and interbead repulsion between unlike beads on the patterns found. Figure S2 summarizes the effect of surfactant length. Figures S3 and S4 illustrate the effect of SAM stoichiometry for low and high interbead repulsion between unlike surfactants, respectively. This material is available free of charge via the Internet at http://pubs.acs.org.

REFERENCES AND NOTES

1. Jackson, A. M.; Myerson, J. W.; Stellacci, F. Spontaneous Assembly of Subnanometre-Ordered Domains in the Ligand Shell of Monolayer-Protected Nanoparticles. *Nat. Mater.* **2004**, *3*, 330–336.
2. Jackson, A. M.; Hu, Y.; Silva, P. J.; Stellacci, F. From Homoligand- to Mixed-Ligand-Monolayer-Protected Metal Nanoparticles: A Scanning Tunneling Microscopy Investigation. *J. Am. Chem. Soc.* **2006**, *128*, 11135–11149.
3. Centrone, A.; Hu, Y.; Jackson, A. M.; Zerbi, G.; Stellacci, F. Phase Separation on Mixed-Monolayer-Protected Metal Nanoparticles: A Study by Infrared Spectroscopy and Scanning Tunneling Microscopy. *Small* **2007**, *5*, 814–817.
4. DeVries, G. A.; Brunnbauer, M.; Hu, Y.; Jackson, A. M.; Long, B.; Neltner, B. T.; Uzun, O.; Wunsch, B. H.; Stellacci, F. Divalent Metal Nanoparticles. *Science* **2007**, *315*, 358–361.
5. Uzum, O.; Hu, Y.; Verma, A.; Chen, S.; Centrone, A.; Stellacci, F. Water-Soluble Amphiphilic Gold Nanoparticles with Structured Ligand Shells. *Chem. Commun.* **2008**, 196–198.
6. Verma, A.; Uzun, O.; Hu, Y.; Hu, Y.; Nan, H.; Watson, N.; Chen, S.; Irvine, D. J.; Stellacci, F. Surface-Structure-Regulated Cell-Membrane Penetration by Monolayer-Protected Nanoparticles. *Nat. Mater.* **2008**, *7*, 588–595.
7. Centrone, A.; Penzo, E.; Sharma, M.; Myerson, J. W.; Jackson, A. M.; Marzari, N.; Stellacci, F. The Role of Nanostructure in the Wetting Behavior of Mixed-Monolayer-Protected Metal Nanoparticles. *Proc. Natl. Acad. Sci.* **2008**, *105*), 9886–9891.
8. Singh, C.; Ghorai, P. K.; Horsch, M. A.; Jackson, A. M.; Larson, R. G.; Stellacci, F.; Glotzer, S. C. Entropy-Mediated Patterning of Surfactant-Coated Nanoparticles and Surfaces. *Phys. Rev. Lett.* **2007**, *99*, 226106.
9. Carney, R. P.; DeVries, G. A.; Dubois, C; Kim, H; Kim, J. Y.; Singh, C; Ghorai, P. K.; Tracy, J. B.; Stiles, R. L.; Murray, R. W.; *et al*. Size Limitations for the Formation of Ordered Striped Nanoparticles. *J. Am. Chem. Soc.* **2008**, *130*, 798–799.
10. Singh, C.; Jackson, A. M.; Stellacci, F.; Glotzer, S. C. Exploiting Substrate Stress to Modify Nanoscale SAM Patterns. *J. Am. Chem. Soc.* **2009**, *131*, 16377–16379.
11. Kuna, J. J.; Voïtchovsky, K.; Singh, C.; Jiang, H.; Mwenifumbo, S.; Ghorai, P. K.; Stevens, M.M.I; Glotzer, S. C.; Stellacci, F. The Effect of Nanometer-Scale Structure on Interfacial Energy. *Nat. Mater.* **2009**, *8*, 837–842.
12. Santos, A.; Singh, C.; Glotzer, S. C. Coarse-Grained Models of Tethers for Fast Self-Assembly Simulations. *Phys. Rev. E* **2010**, *81*, 011113.
13. Singh, H.; Hu, Y.; Khanal, B. P.; Zubarev, E. R.; Stellacci, F.; Glotzer, S. C. Striped Nanowires and Nanorods from Mixed SAMs. *Nanoscale* **2011**, *3*, 3244–3250.
14. Pons-Siepermann, I. C.; Glotzer, S. C. Design of Patchy Particles Using Ternary Self-Assembled Monolayers. *Soft Matter*, in press, **2012**, DOI:10.1039/C2SM00014H.
15. Ingram, R. S.; Hostetler, M. J.; Murray, R. W. Poly-hetero-ω-Functionalized Alkanethiolate-Stabilized Gold Cluster Compounds. *J. Am. Chem. Soc.* **1997**, *119*, 9175–9178.
16. Singh, C. Ph.D. Thesis, University of Michigan, 2010.
17. Groot, R. D.; Warren, P. B. Dissipative Particle Dynamics: Bridging the Gap Between Atomistic and Mesoscopic Simulation. *J. Chem. Phys.* **1997**, *107*, 4423–4435.
18. HOOMD-blue Web page: http://codeblue.umich.edu/hoomd-blue.
19. Anderson, J. A.; Lorenz, C. D.; Travesset, A. General Purpose Molecular Dynamics Simulations Fully Implemented on Graphics Processing Units. *J. Comput. Phys.* **2008**, *227*, 5342–5359.
20. Phillips, C. L.; Anderson, J. A.; Glotzer, S. C. Pseudo-Random Number Generation for Brownian Dynamics and Dissipative Particle Dynamics Simulations on GPU Devices. *J. Comput. Phys.* **2011**, *230*, 7191–7201.